International Journal of Enhanced Research in Medicines & Dental Care (IJERMDC),
ISSN: 2349-1590, Vol. 12 Issue 3, March-2025

Formulation Development and In Vitro Evaluation of Transmucosal Drug Delivery of Rizatriptan Liposomes

V. Yamuna[1], Ch Sreenivasa Kumari[2], V Phani Deepthi[3]

[1,2,3]Department of Pharmaceutics, JNTUA-Oil Technological and Pharmaceutical Research Institute

ABSTRACT

Rizatriptan, a potent antimigraine agent, suffers from low bioavailability (45-47%) due to extensive hepatic first-pass metabolism when administered orally. To overcome this limitation, this study aimed to develop and evaluate brain-targeted liposomal formulations of rizatriptan for nasal transmucosal delivery. Glutathione (GSH)-conjugated liposomes were designed to enhance brain delivery by bypassing the blood-brain barrier (BBB) and leveraging the olfactory pathway. Liposomes were prepared using the thin-film hydration method and characterized for particle size, zeta potential, entrapment efficiency, and in-vitro drug release. The optimized formulations were evaluated for in-vivo pharmacokinetics and brain targeting efficiency in rats. Results demonstrated that GSH-conjugated liposomes significantly improved brain delivery of rizatriptan, with enhanced pharmacokinetic parameters and stability over 12 months. The nasal route, combined with liposomal delivery, offers a promising alternative to oral administration for the treatment of migraines and other CNS disorders.

INTRODUCTION

Migraine is a debilitating neurological disorder affecting millions worldwide. Rizatriptan, a selective 5-HT1D receptor agonist, is commonly used for migraine treatment. However, its oral administration is limited by low bioavailability (45-47%) due to extensive hepatic first-pass metabolism. Nasal transmucosal drug delivery offers a promising alternative, providing non-invasive, rapid drug absorption and direct delivery to the brain via the olfactory pathway, bypassing the BBB.

Liposomes, lipid-based vesicles, have shown potential in crossing biological membranes, including the BBB. Cholesterol, an integral component of liposomes, provides rigidity and stability. Conjugation of cholesterol with glutathione (GSH), a natural antioxidant abundant in the brain, enhances brain targeting. This study aimed to develop and evaluate GSH-conjugated liposomal formulations of rizatriptan for nasal delivery, focusing on overcoming the limitations of oral administration and enhancing brain delivery.

MATERIALS AND METHODS

Rizatriptan, cholesterol, Lipoid S 100, glutathione, and other excipients were procured from Sigma-Aldrich. All solvents and reagents were of analytical grade.

Synthesis of Cholesterol-GSH Conjugate:
Cholesterol acrylate was synthesized and conjugated with glutathione using a chemical reaction scheme. The conjugate was characterized using FTIR and H1NMR.

Preparation of Liposomes:
Liposomes were prepared using the thin-film hydration method. Two types of liposomes were prepared: non-conjugated (F1-F9) and GSH-conjugated (G1-G9).

Formulation Table:

Table 1 : Formulation Table

Formulation code	Rizatriptan (mg)	CHL (mg)	CHL-GSH conjugate (mg)	Lipoid S 100 (mg)	PEG 400 (ml)	Benzalkonium chloride (ml)	Phosphate buffer q.s. (ml)
F1	10	150	-	75	2	0.1	10
F2	10	150	-	100	2	0.1	10
F3	10	150	-	125	2	0.1	10
F4	10	300	-	75	2	0.1	10
F5	10	300	-	100	2	0.1	10
F6	10	300	-	125	2	0.1	10
F7	10	450	-	75	2	0.1	10
F8	10	450	-	100	2	0.1	10
F9	10	450	-	125	2	0.1	10
G1	10	-	75	75	2	0.1	10
G2	10	-	100	100	2	0.1	10
G3	10	-	125	125	2	0.1	10
G4	10	-	75	75	2	0.1	10
G5	10	-	100	100	2	0.1	10
G6	10	-	125	125	2	0.1	10
G7	10	-	75	75	2	0.1	10
G8	10	-	100	100	2	0.1	10
G9	10	-	125	125	2	0.1	10

RESULTS AND DISCUSSIONS

Characterization of drug

Melting point

Melting point of rizatriptan was found to be 179^0C which matches with the reference value.

UV-Vis spectrophotometry

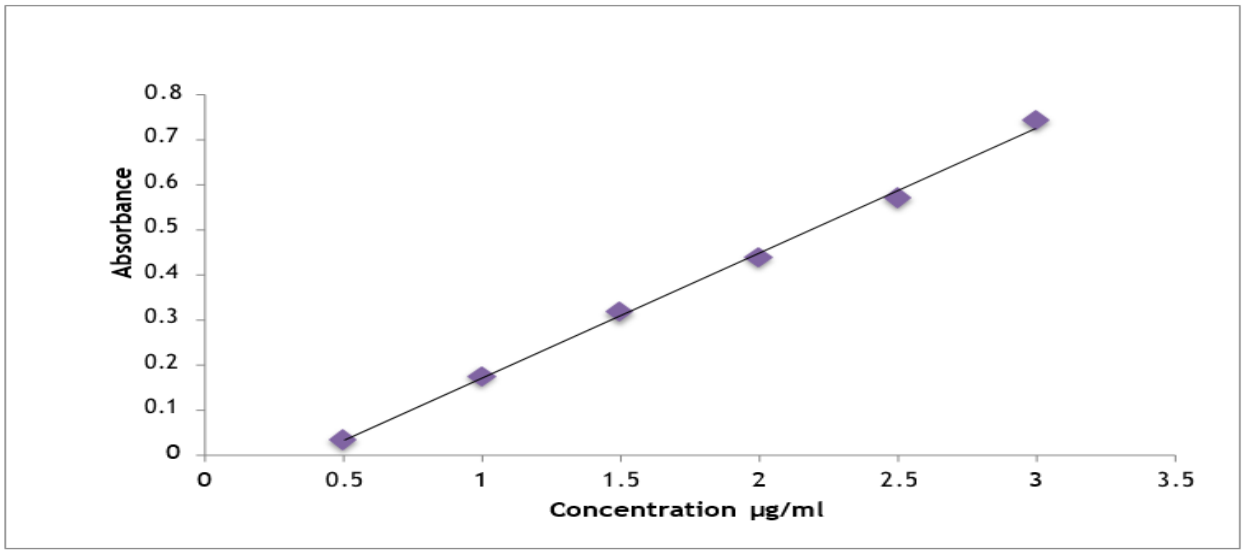

Figure 1: Calibration curve of rizatriptan in phosphate buffer pH 6.6.

FTIR studies

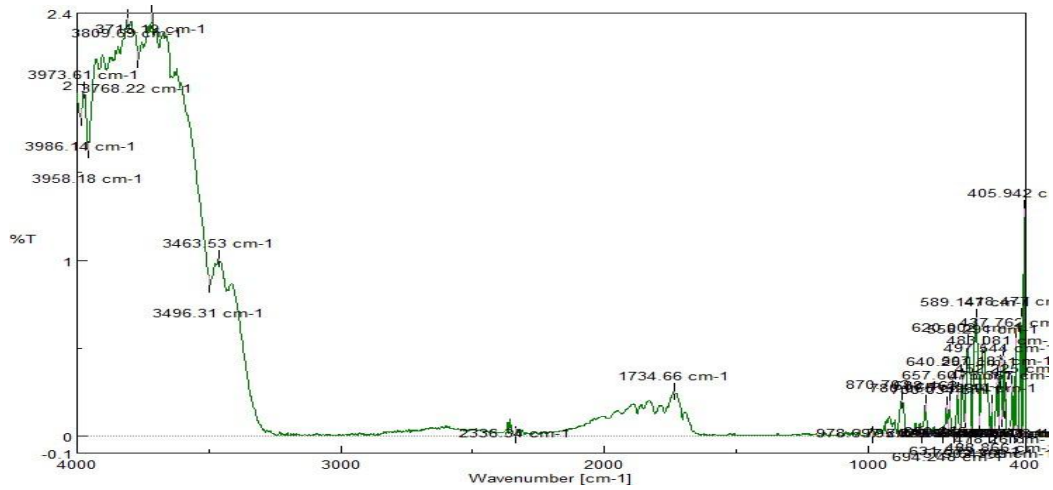

Figure 2: FTIR spectrum of rizatriptan.

Differential Scanning Calorimetry

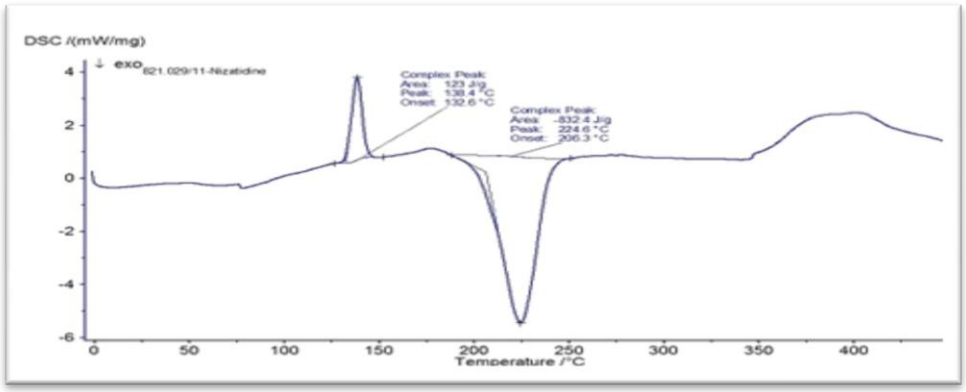

Figure 3 DSC thermogram of Rizatriptan

HPLC

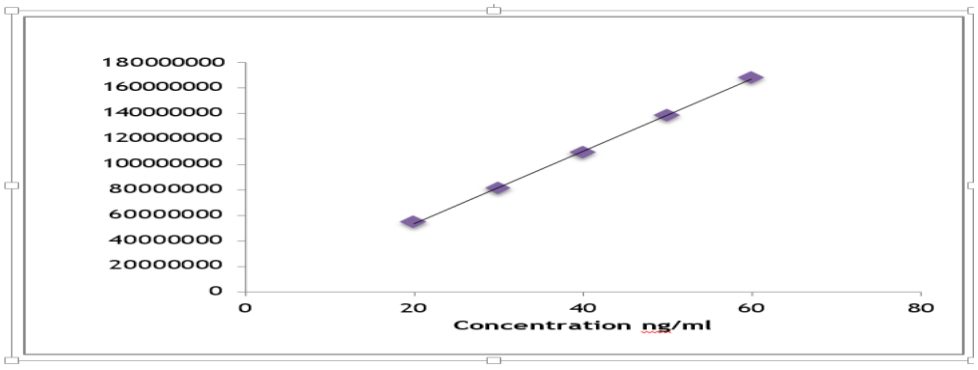

Figure 4: Calibration Curve For Rizatriptan By HPLC

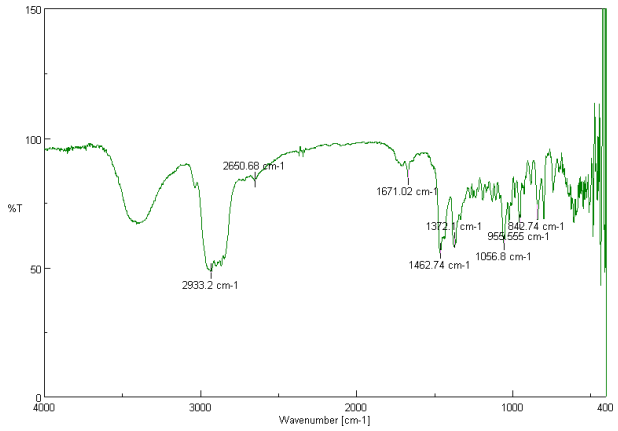

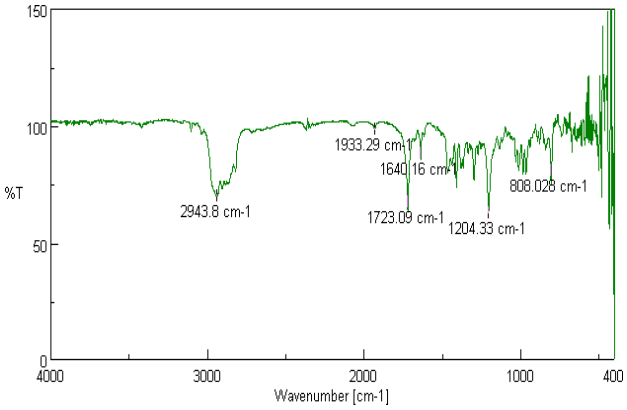

Figure 5: FTIR spectrum of cholesterol

Figure 6: FTIR spectrum of cholesterol Acrylate

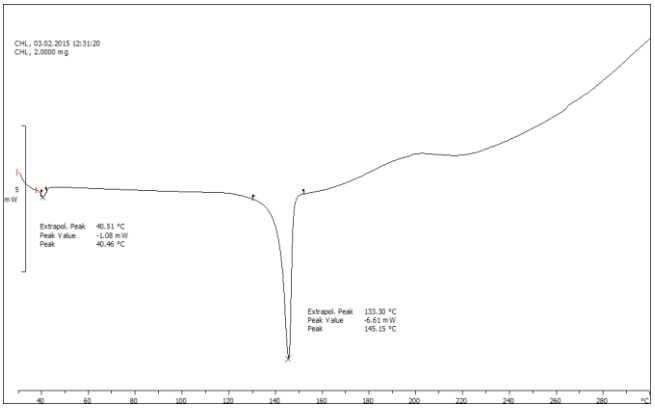

Figure 9: DSC thermogram of cholesterol

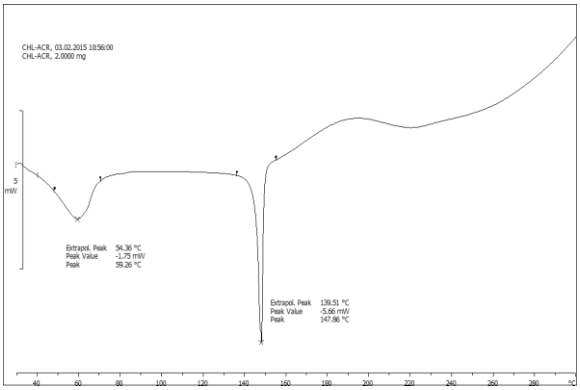

Figure 10: DSC thermogram of cholesterol acrylate

Characterization of cholesterol-GSH conjugate

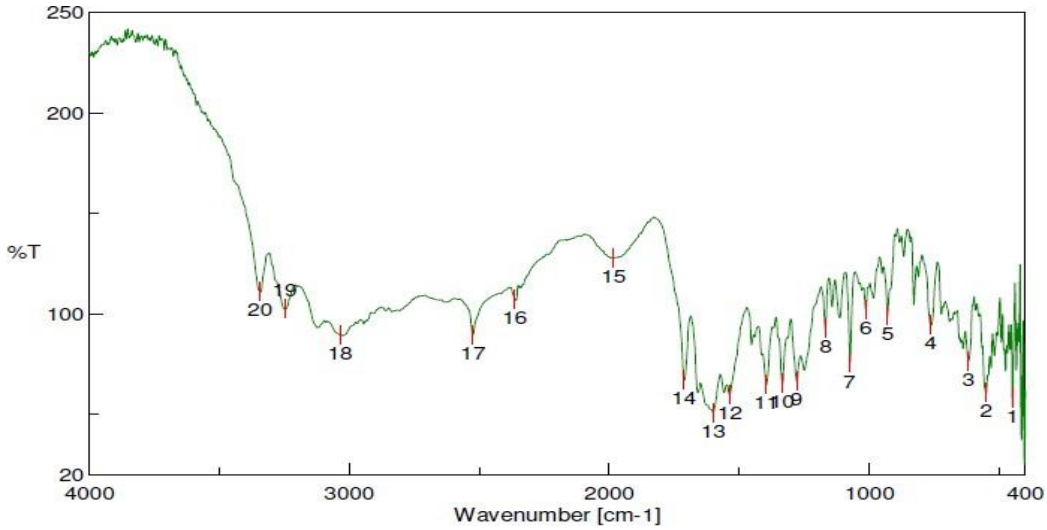

Figure 11: FTIR spectrum of Glutathione

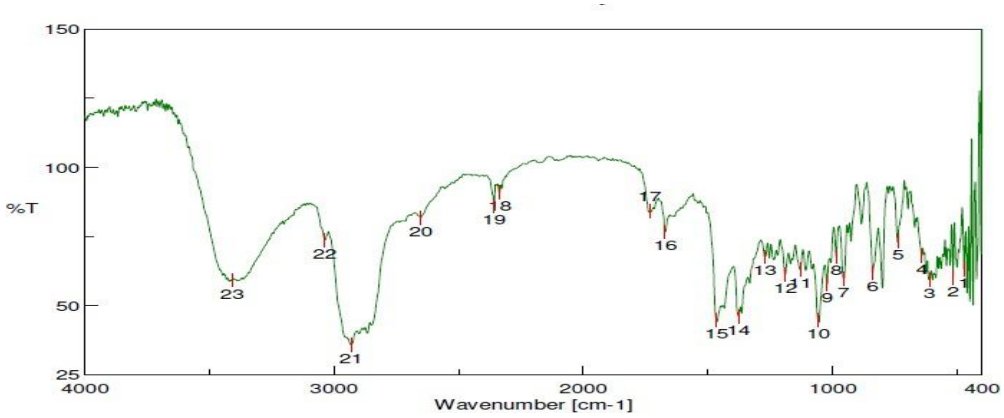

Figure 12: FTIR spectrum of cholesterol-glutathione conjugate

Evaluation of liposomes

Table 2: Evaluation of liposomes formulations

Formulation	Zeta Potential mV	Particle size Nm	PDI	Entrapment efficiency %	In-vitro drug release %
F1	40.34	290	0.31	81.5	75.3
F2	34.54	380	0.36	85.2	66.1
F3	42.9	181	0.45	88.1	90.2
F4	41.51	245	0.42	76.3	87.3
F5	36.53	355	0.4	82.4	69
F6	44.6	470	0.34	92.1	61.1
F7	49.04	195	0.37	70.7	80.2
F8	47.09	280	0.5	78	70
F9	36.54	540	0.4	80.6	59.3
G1	48.34	305	0.43	78.2	72
G2	39.54	402	0.36	82.3	62
G3	45.9	194	0.5	84.9	86.4
G4	37.51	272	0.35	72.4	83.4
G5	46.53	370	0.3	79.2	66.2
G6	47.6	490	0.38	88	57.1
G7	36.04	220	0.49	66	78.1
G8	45.09	291	0.46	75.2	66.4
G9	39.54	590	0.32	77.5	56.2

Particle size, zeta potential and PDI

Figure 14: Response surface and contour diagram for effect of Lipoid S 100 and cholesterol on particle size for non conjugated liposome formulations.

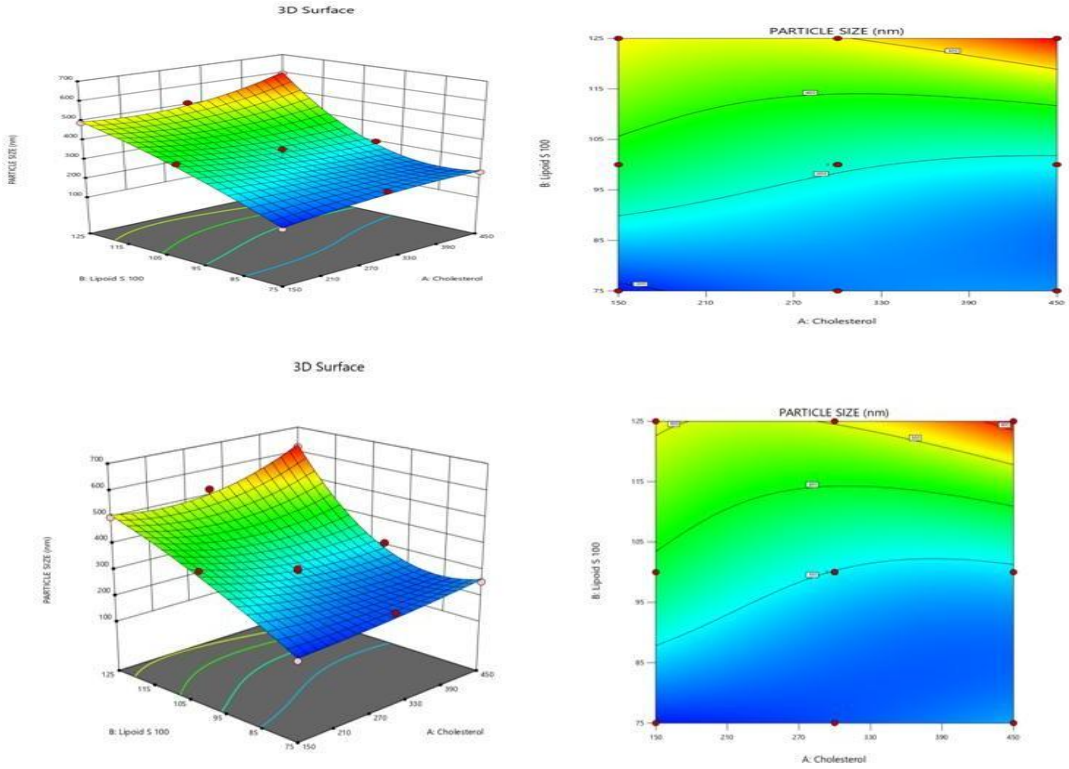

Figure 15: Response surface and contour diagram for effect of Lipoid S 100 and GSH conjugated cholesterol on particle size of liposome.

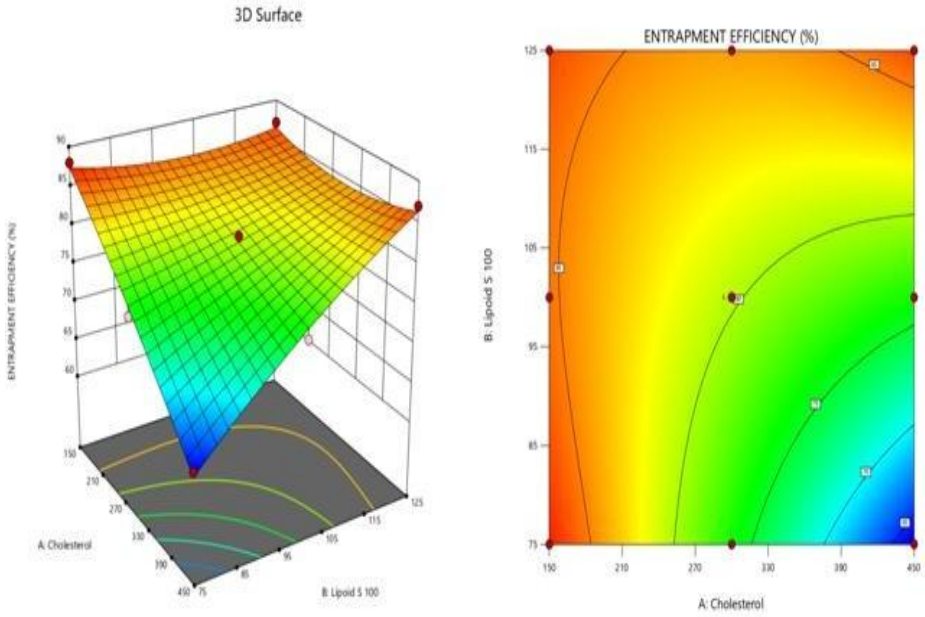

Figure 16: Response surface and contour diagram for effect of Lipoid S 100 and cholesterol on entrapment efficiency for non conjugated liposomes.

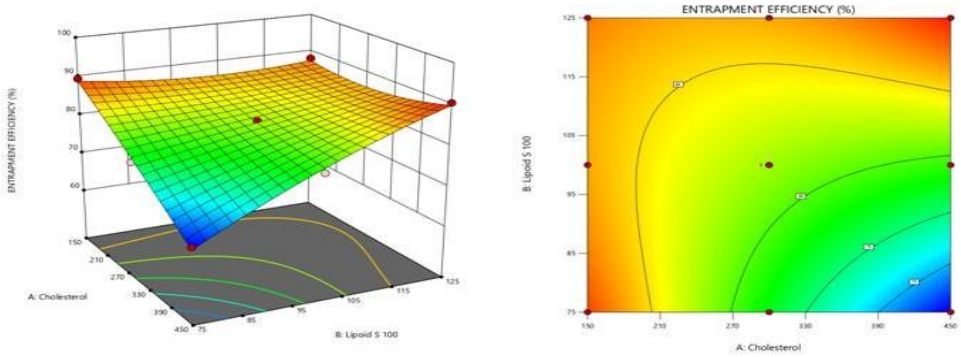

Figure 17: Response surface and contour diagram for effect of Lipoid S 100 and GSH conjugated cholesterol on entrapment efficiency of liposomes.

In-vitro drug releas

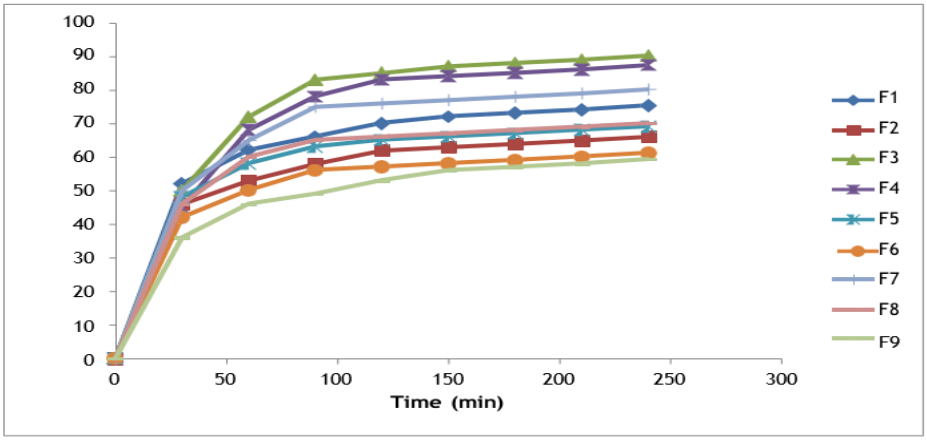

Figure 18: In vitro drug release for non conjugated liposomes

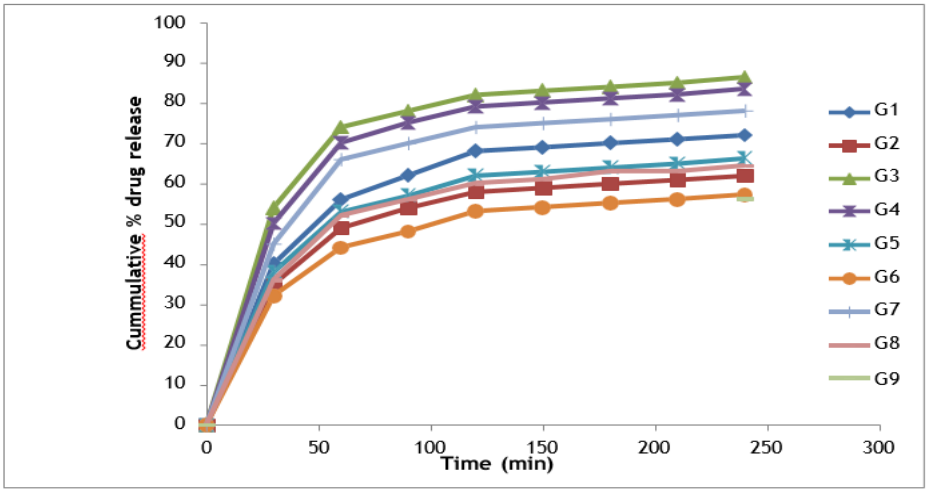

Figure 19: In vitro drug release for glutathone conjugated liposomes formulations.

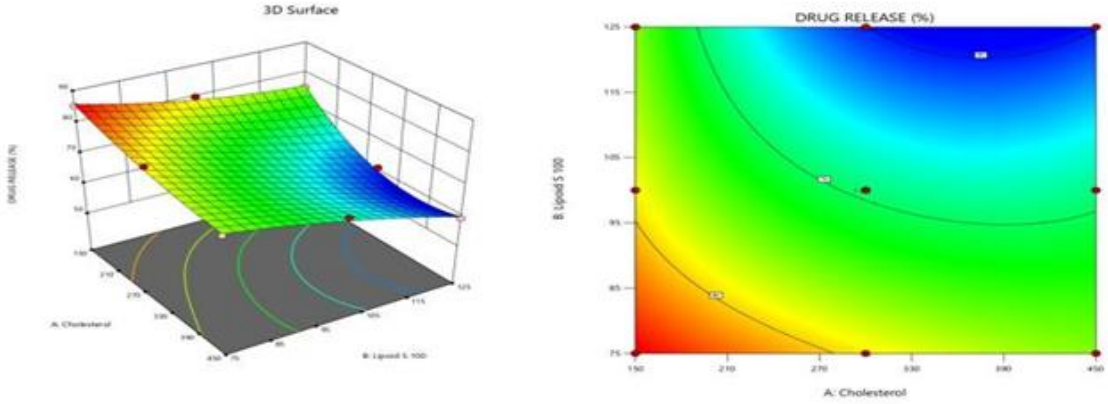

Figure 19: Response surface and contour diagram for effect of Lipoid S 100 and cholesterol on drug release for non conjugated liposomes.

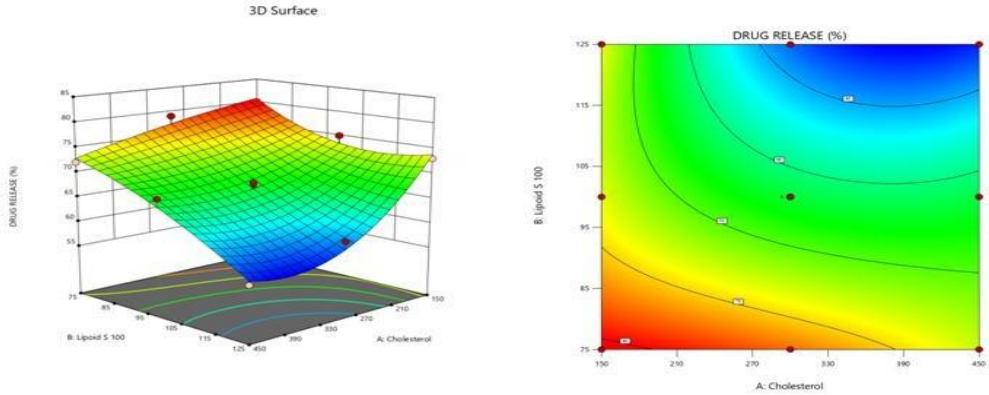

Figure 20: Response surface and contour plots for effects of GSH conjugated cholesterol and Lipoid S100 on drug release.

STATISTICAL ANALYSIS

Liposomes with non conjugated cholesterol

Table 4: ANOVA for non conjugated liposome formulation.

Models	R^2	Adeq Precision	Model F Value	p Value
Particle size				
Cubic	0.993	39.74	129.41	0.001
***In vitro* drug release**				
Cubic	0.984	21.35	125.36	0.001
Entrapment efficiency				
Cubic	0.978	35.35	122.98	0.001

Mathematical Models

Particle size =
$359.27+50A+112.5B+113.5AB+39.96A^2-12.46B^2-53.5A^2B+116AB^2$
In vitro drug release =
$68.58-1.95A-13.1B-8.95AB+0.49A^2+6.64B^2-8.45AB^2$

Entrapment efficiency =
$82.83-3.6A+7.9B+0.825AB-2.33A^2+0.26B^2-3.77A^2B-0.07AB^2$

Where A= cholesterol, B= Lipoid S100

Table 5: Evaluation of optimized formulation

Particle size nm		Entrapment efficiency %		In-vitro drug release %	
Predicted	**Observed**	**Predicted**	**Observed**	**Predicted**	**Observed**
187.76	181	88.9	88.1	88.8	86.4

ANOVA

Table 6: ANOVA for CHL-GSH conjugated liposomes

Models	R^2		Adeq Precision	Model F Value	p Value
	Particle size				
Cubic	0.989		40.2	135.2	0.001
	***In vitro* drug release**				
Cubic	0.979		23.6	140.3	0.001
	Entrapment efficiency				
Cubic	0.992		38.2	150.3	0.001
	Regression equations of the fitted model Particle size = $298.66+44.5A+139B+14.75AB+36.21A^2+67.71B^2+28.75A^2B+89.25AB^2$ *In vitro* drug release = $66.83-3.51A-9.5B-2.25AB+3.1A^2+1.1B^2+3.75A^2B-2.75AB^2$ Entrapment efficiency = $80.28-4.5A+4B+6AB+0.5345A^2+0.0345B^2+1.5A^2B-1.5AB^2$ Where A= glutathione conjugated cholesterol, B= Lipoid S100				

Optimization of liposomes with glutathione conjugated cholesterol

Table 7: Evaluation of optimized formulation

Particle size Nm		Entrapment efficiency %		In-vitro drug release %	
Predicted	**Observed**	**Predicted**	**Observed**	**Predicted**	**Observed**
204.81	194	86.34	84.9	86.78	90.2

Scanning electron microscopy:

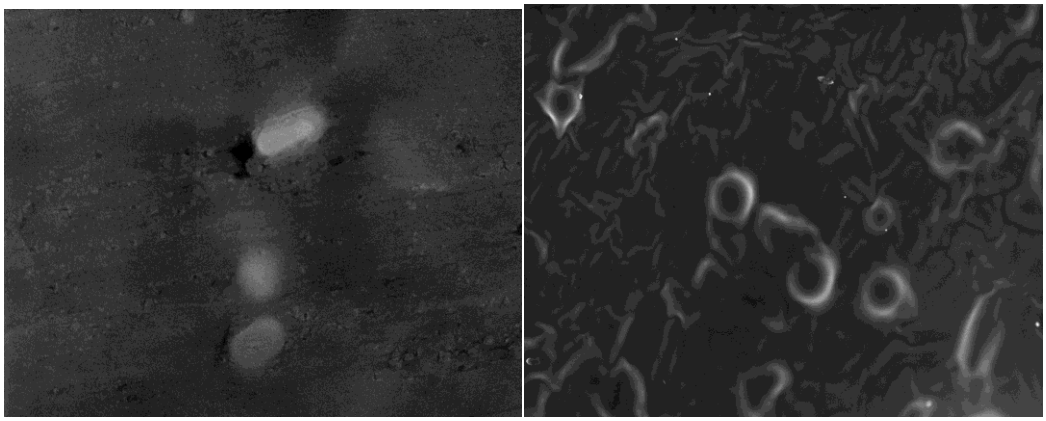

(a) **(b)**

Figure 21: Scanning electron microscopic image of (a) non- conjugated liposomes and (b) CHL-GSH conjugated liposomes.

Stability studies

Table 8 : Stability studies for GSH conjugated liposome formulation of rizatriptan

Testing Period (month(	Entrapped Drug Content (%)	Particle Size (nm)	Zeta Potential (mV)	Invitro drug release (%)	pH
0	86.5±0.81	196±2.1	5.9±0.1	88.3±0.92	6.4±0.08
1	86.1±0.84	197±2.3	5.4±0.3	87.6±0.73	6.3±0.03
3	84.6±0.78	199±1.9	5.6±0.2	87.1±0.54	6.5±0.07
6	84.1±0.68	202±2.4	5.5±0.1	85.2±0.84	6.2±0.05
12	83.3±0.92	203±2.5	5.7±0.4	84.1±0.89	6.3±0.04

CONCLUSION

The study successfully demonstrated that GSH-conjugated liposomes significantly enhance the brain delivery of Rizatriptan via the nasal route. The optimized liposomal formulations showed improved pharmacokinetic parameters, higher brain concentrations, and excellent stability. The use of GSH as a targeting ligand proved effective in enhancing brain targeting efficiency, making it a promising approach for the treatment of migraines and other CNS disorders. The nasal route, combined with liposomal delivery, offers a viable alternative to oral administration, bypassing first-pass metabolism and achieving faster and higher drug concentrations in the brain.

REFERENCES

[1]. Abhang P, Momin M, Inamdar M, Kar S. Transmucosal Drug Delivery- An Overview. Drug Delivery Letters. 2014; 4:26-37.
[2]. Akbarzadeh A, Rezaei-Sadabady R, Davaran S. Liposome: classification, preparation, and applications. Nanoscale Research Letters. 2013; 8(1):102.
[3]. Akoglu E, Gorur S, Atik E, Okuyucu S, Sangun O. Effect of 1- deamino 8- D -arginine vasopressin spray on nasal cytology and mucociliary clearance in patients with nocturnal enuresis. International Journal of Pediatric Otorhinolaryngology. 2006; 70:1919—1922.
[4]. Alpar H, Eyles J, Williamson E, Somavarapu S. Intranasal vaccination against plague, tetanus and diphtheria. Advanced Drug Delivery Reviews. 2001; 51:173-201.
[5]. Alsarra I, Hamed A, Alanazi F. Acyclovir liposomes for intranasal systemic delivery: development and pharmacokinetics evaluation. Drug Delivery. 2008; 15:313-321.
[6]. Alsarra I, Hamed A, Alanazi F, El Maghraby G. Vesicular Systems for Intranasal Drug Delivery. In: Jain K. (Eds) Drug Delivery to the Central Nervous System. Neuromethods, Humana

Press. 2010.
[7]. Alsarra I, Hamed A, Mahrous G, El Maghraby G, Al-Robayan A, Alanazi F. Mucoadhesive polymeric hydrogels for nasal delivery of Acyclovir. Drug Development and Industrial Pharmacy. 2009; 35:352-62.
[8]. Andresen, T, Jensen S, Jorgensen, K. Advanced strategies in liposomal cancer therapy: Problems and prospects of active and tumor specific drug release. Progress in Lipid Research. 2005; 44(1):68–97.
[9]. Arora P, Sharma S, Garg S. Permeability issues in nasal drug delivery. Drug Discovery Today. 2002; 7(18):967-975.
[10]. Asli-Sahin-Yilmaz, Naclerio R. Anatomy and physiology of the upper airway. Proceedings of the American Thoracic Society. 2011; 8:31–39.
[11]. Baker H, Spencer R. Transneuronal transport of peroxidase- conjugated wheat germ agglutinin (WGA–HRP) from the olfactory epithelium to the brain of the adult rat. Experimental Brain Research. 1986; 63:461–473.
[12]. Bommer R. Drug Delivery – Nasal Route. In: J.C.B. James S, Encycolopedia of Pharmaceutical Technology. New York: Marcel Dekker; 1998. Vol 1, p. 854-862.
[13]. Brooking J, Davis S, Illum L. Transport of nanoparticles across the rat nasal mucosa. Journal of Drug Targeting. 2001; 9:267–279.
[14]. Chavanpatil M, Vavia P. Nasal drug delivery of sumatriptan succinate. Pharmazie. 2005; 60(5):347-349.
[15]. Chien Y, Su K, Chang S. Anatomy and physiology of the nose. In: Chien Y, Su K ,Chang S (Eds.). Nasal Systemic Drug Delivery. New York: Marcel Dekker Inc. 1989; p.1-26.
[16]. Corbo D, Liu J, Chien Y. Characterization of the barrier properties of mucosal membranes. Journal of Pharmaceutical Sciences.1990; 79:202-206.